Electron-Induced Upsets and Stuck Bits in SDRAMs in the Jovian Environment

Daniel Söderström, Lucas Matana Luza, Heikki Kettunen, Arto Javanainen, Wilfrid Farabolini, Antonio Gilardi, Andrea Coronetti, Christian Poivey, Luigi Dilillo

Title: Electron-Induced Upsets and Stuck Bits in SDRAMs in the Jovian Environment

Author(s): Daniel Söderström, Lucas Matana Luza, Heikki Kettunen, Arto Javanainen, Wilfrid Farabolini, Antonio Gilardi, Andrea Coronetti, Christian Poivey, and Luigi Dilillo

DOI: 10.1109/TNS.2021.3068186

Published: 23 March 2021

Document version: Post-print version (Final draft)

Please cite the original version:
D. Söderström et al., "Electron-Induced Upsets and Stuck Bits in SDRAMs in the Jovian Environment," in IEEE Transactions on Nuclear Science, vol. 68, no. 5, pp. 716-723, May 2021, doi: 10.1109/TNS.2021.3068186.

Electron-Induced Upsets and Stuck Bits in SDRAMs in the Jovian Environment

Daniel Söderström, *Student Member, IEEE,* Lucas Matana Luza, *Student Member, IEEE,* Heikki Kettunen, *Member, IEEE,* Arto Javanainen, *Member, IEEE,* Wilfrid Farabolini, Antonio Gilardi, Andrea Coronetti, *Student Member, IEEE,* Christian Poivey, *Member, IEEE* and Luigi Dilillo, *Member, IEEE*

Abstract

This study investigates the response of synchronous dynamic random access memories to energetic electrons, and especially the possibility of electrons to cause stuck bits in these memories. Three different memories with different node sizes (63, 72 and 110 nm) were tested. Electrons with energies between 6 MeV and 200 MeV were used at RADEF in Jyväskylä, Finland, and at VESPER in CERN, Switzerland. Photon irradiation was also performed in Jyväskylä. In these irradiation tests, stuck bits originating from electron-induced single event effects were found, as well as single bit-flips from single electrons. To the best knowledge of the authors, this is the first time that stuck bits from single electron-events has been reported in the literature. It is argued in the paper that the single event bit-flips and stuck bits are caused by the same mechanism, large displacement damage clusters, and that they represent different amounts of damage to the memory cell. After a large particle fluence, a rapid increase in the error rate was observed, originating from the accumulation of smaller displacement damage clusters in the memory cells. The 110 nm memory was a candidate component to fly on the ESA JUICE mission, so the single event effect cross section as a function of electron energy was compared to the expected electron environment encountered by JUICE to estimate the error rates during the mission.

Index Terms

Electron radiation, radiation effects, single event upsets, stuck bits, total ionizing dose

I. Introduction

RADIATION effects in electronic components caused by energetic electrons is of higher concern in the Jovian radiation environment than in the radiation belts surrounding Earth, due to the harder energy spectrum present around Jupiter [1]–[3]. This study is motivated by the European Space Agency's (ESA) JUpiter ICy moons Explorer (JUICE) mission in the Jovian environment, and focuses on electron-induced radiation effects in synchronous dynamic random access memories (SDRAM), where one of the tested components was a candidate to be used on board JUICE.

One of the main points of interest of this work was to investigate the possibility of stuck bits being induced by single electrons. This has, to the best of the authors' knowledge, not previously been observed or reported.

Previous studies of single event effects (SEE) caused by energetic electrons have been reported in e.g. [4]–[9], where single event upsets (SEU) and single event latch-up (SEL) were investigated mainly in static random access memories (SRAM). In [4] SEUs from secondary electrons induced by X-rays were studied, while in [5] and [6] SEUs in FPGA embedded and configuration RAM were studied. In [7] SEUs in SRAMs operated at a low voltage were observed. SEUs from high energy electrons were studied in [8], and the same authors studied electron-induced SEL in [9].

In this work concerning SDRAM, stuck bits are defined as bits with reoccurring errors, so that the memory cell is returning the same data when it is read ('0' or '1'), independent of the value which was written to the cell. This

Manuscript submitted October 1, 2020.

The results presented here are part of the RADSAGA project that has received funding from the European Union's Horizon 2020 research and innovation program under the Marie Sklodowska-Curie grant agreement No 721624.

This work was also supported by the European Space Agency (ESA) under contract 4000124504/18/NL/KML/zk, the Van Allen Foundation under contract no. UM 181387, and Region Occitane under contract no. UM 181386.

D. Söderström, H. Kettunen, A. Javanainen and A. Coronetti are with the Department of Physics at the University of Jyväskylä, Finland. Contact: daniel.p.soderstrom@jyu.fi.

L. Matana Luza and L. Dilillo are with Laboratoire d'Informatique, de Robotique et de Microélectronique de Montpellier (LIRMM), Montpellier, France.

A. Javanainen is also with the Electrical Engineering and Computer Science Department at Vanderbilt University, Nashville, TN 37235, USA.

A. Gilardi is with the University of Napoli Federico II, DIETI, Napoli, Italy.

W. Farabolini, A. Gilardi and A. Coronetti are with CERN, Geneva, Switzerland.

C. Poivey is with the European Space Agency, ESTEC, Noordwijk, The Netherlands

Thanks to ESA and 3D+ for providing memory samples tested in this work.

TABLE I
SUMMARY OF SPECIMEN USED IN THE EXPERIMENTS.

Memory	Node size (nm)	DUT IDs
IS42S86400B	110	SDF1, SDF3, SDF4, SDF5, SDG1, SDG3, SDG4, SDG5, SDG6
IS42S16320D	72	SDB1
IS42S16320F	63	SDE1

behaviour is different from typical SEU, which manifest themselves as a bit-flip, only present in a single reading of the bit in question, but not in any consecutive reads of the cell after it had been rewritten.

Stuck bits in SDRAM have been studied in irradiation experiments using different particle species, such as protons and ions, e.g. in [10]–[13]. There, a common suggested cause for the stuck bits is single particles creating leakage paths from the cell capacitor by displacement damage. In [13], as well as in [14], [15], intermittently stuck bits (ISB) are discussed, which deals with the phenomenon of bits appearing as stuck in some periods of time, when otherwise they can operate normally and return the correct value which was written to the memory cell. Stuck bits are discussed in [16] under the terminology weakened cells, where flight data and ground data are presented. Here displacement damage from single particles is also identified as the cause for the upsets.

In this paper, experimental SEE results from electrons, resulting in stuck bits and bit-flips are presented and discussed. No new interpretation of the mechanism causing stuck bits or ISBs in SDRAMs is presented, but the cause of stuck bits is put in relation to that of single bit-flips. The degradation of the cells subject to SEE is studied, and implications of the usage of the studied SDRAM in the JUICE mission are discussed.

II. TESTED COMPONENTS AND EXPERIMENTAL PROCEDURE

The tested components are described in Table I, where the ISSI 512 Mb SDRAM IS42S86400B [17] was a candidate to be flown on the JUICE mission when the irradiation tests were performed.

The tested memory devices were all ISSI 512 Mb Single Data Rate (SDR) SDRAMs, with 536,870,912 bits separated on four banks. The IS42S86400B memory banks are organized into 8192 rows by 2048 columns of 8 bits, while the IS42S16320D/F [18], [19] memories have 8192 rows of 1024 columns by 16 bits in their banks. They all have an operating frequency of up to 143 MHz, with a 3.3 V bias, and were packaged in 54-pin TSOP-II packages. None of the devices were delidded for the irradiation experiments, and no further information about the memory layout in terms of physical structure or physical mapping of the memory bits are known to the authors.

A Terasic DE0-CV FPGA development board [20] was used as a memory control board during the experiments, and the samples were mounted on daughter boards connected to the control board through a GPIO pin interface. Only the device under test (DUT) was placed in the radiation field during irradiation, and the control board was kept outside the beam.

The components were running dynamic tests during irradiation, with read and write operations carried out continuously. The memories were running a March C- test, which was slightly modified so that it would not have any stand-alone write or read elements [21]. The dynamic test cycle of read and write operations for the DUTs during irradiation is shown in (1).

$$\begin{aligned} \uparrow (w0); \{ &\uparrow (r0, w1); \uparrow (r1, w0); \\ &\downarrow (r0, w1); \downarrow (r1, w0) \} \end{aligned} \tag{1}$$

The operations within the brackets $\{\ \}$ in (1) were looped over during irradiation, the *r* and *w* are read and write operations respectively, the '0' and '1' are data patterns of all '0' and all '1', and the arrows represent the address accessing order in the operation, starting from either the lowest address and stepping upwards ($\uparrow$), or vice versa ($\downarrow$). The IS42S86400B memories were operated at 100 MHz, while the IS42S16320D/F memories were operated at 75 MHz, because the D/F memories could not operate without issues at higher frequencies with the cabling and set-up used in the experiment. During all runs, the memories were operated with their nominal refresh frequency 128 kHz. This frequency is based on the auto refresh command, which automatically defines the row address to refresh. At 128 kHz, this command is executed 8192 times every 64 ms [17] so that every row of the memory is refreshed once per 64 ms. This refresh frequency was altered during analysis procedures to investigate data retention times of the memories' bits.

III. TEST FACILITIES

The tests with high-energy electrons (60 - 200 MeV) were performed at VESPER (the Very energetic Electron facility for Space Planetary Exploration missions in harsh Radiative environments) [22] at CERN (The European

Organization for Nuclear Research). Lower energy electron (up to 20 MeV) and photon exposures were performed at RADEF (RADiation Effects Facility) at the University of Jyväskylä, Finland, with a Varian Clinac (Clinical LINear ACcelerator) 2100 CD [23].

A. VESPER

The VESPER beam is pulsed, and the electrons arrive in short bunches (< 10 ps) at a frequency of 3 GHz. The electron bunches were arranged in trains of 100 electron bunches each, and the trains were arriving at a 10 Hz frequency.

A beam current transformer (BCT) was used to monitor the beam current during the runs, and an Yttrium Aluminium Garnet (YAG) screen was used to monitor the beam spot shape. A camera was filming the scintillating YAG-screen to monitor the beam profile during the run. The beam spot was approximated to be of Gaussian shape, and the shape parameters of the beam centre and standard deviation ($\mu_{x,y}$ and $\sigma_{x,y}$) were logged in real time while performing the experiment.

This system for beam monitoring worked rather well with a high intensity beam. As the beam intensity gets lower, and as the beam energy gets lower, the beam profile and charge is monitored less efficiently. Since the irradiation was done in air, with the beam having to pass through an exit window as well as a scattering screen to enlarge the beam spot, a more diffuse and scattered beam would reach the scintillating screen when a beam with lower energy and penetration power is used for a given beam intensity. The DUTs were unable to operate under high electron fluxes without large portions of the memory being corrupted, so a rather low flux (in general about $2-3\cdot10^8$ e/cm^2/s, which is low in relation to what the facility could provide) had to be chosen. The beam spot was thus rather diffuse, and the exact beam position difficult to recreate. In combination with this, the beam spot was drifting (generally < 5 mm) vertically and horizontally during the runs.

To calculate the electron fluence on the DUT, the beam charge and measured shape ($\sigma_{x,y} = 12-15$ mm depending on beam energy) were used. The fluence on the DUT was assumed as the average fluence within the area $\sigma_x \times \sigma_y$ and with an estimated uncertainty 20 % due to drifting of the electron beam position during irradiation and the diffuse beam spot.

B. RADEF

Electrons with energies of 6, 9, 12, 16 and 20 MeV are available at the Clinac at RADEF. This electron beam is also pulsed and consists of 5 µs long pulses every 5 ms (pulse frequency of 200 Hz). Furthermore, the radiation from the machine is provided in runs of up to 10 krad(H_2O) each, so the irradiation has to be restarted every 10 krad(H_2O). This is however a fast procedure, taking only a few seconds of time. 6 MeV and 20 MeV electrons were used for tests discussed in this paper.

The Clinac can be run in electron mode or in photon mode. In photon mode, a target is placed within the electron beam, converting the incident electrons to a bremsstrahlung spectrum of photons. In photon mode, the Clinac can be run at 6 MV or 15 MV, which means that the resulting photon spectrum is that of the bremsstrahlung from electrons accelerated over a 6 MV or 15 MV electric field (electrons with energies 6 MeV and 15 MeV) respectively. The 6 MV mode were used for photon-tests with results presented in this paper.

The photon energy spectrum for the 6 MV operating mode is a smooth continuous distribution from 0 to 6 MeV, with an intensity maximum at about 1 MeV, and can be seen in Fig. 1. The spectrum is the result of a Geant4-simulation [24] where 6 MeV electrons were impinging on a 2.5 mm thick Ta-target. The bremsstrahlung photons generated in the target was transported through a tungsten flattening filter, which is present in the beam line to create a spatially homogeneous photon field, and a 1 m air column, after which the photon energy spectrum was recorded. The sharp peak in the spectrum located at 0.511 MeV consists of annihilation photons.

The beam was monitored with in-beam ionization chambers, which were calibrated against a dosimeter in the beam centre at maximum dose depth in water (i.e., at the water depth where the dose rate is the highest). An IBA PPC40 dosimeter [25] was used for electrons and an IBA FC65-P dosimeter [25] for photons.

At the facility, the dose at maximum dose depth in water is measured and recorded. In addition, the water surface dose was also measured, so the dose rate ratio between the maximum depth and surface is known. From this, the electron fluence on the DUT was calculated as the surface dose in water, divided by the collision stopping power (S_{coll}) in water (using appropriate units). The surface dose factors and S_{coll} for the electron energies used at RADEF are shown in Table II.

When values of deposited dose are presented for electrons in this paper, it is the surface dose in Si. This is calculated from the electron fluence, by multiplying the fluence with S_{coll} in Si for the electron energy in question. For photon irradiation, the surface dose is as seen in Table II much smaller than the dose at maximum dose depth in water. The irradiation with photons was performed with 6 MV photons with the DUT covered by 1.5 cm of acrylic

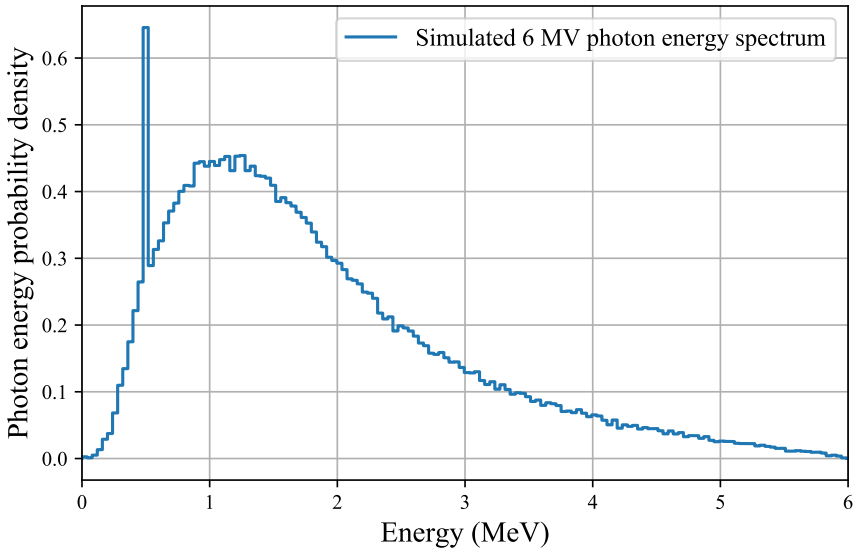

Fig. 1. Simulated photon energy spectrum of the 6 MV photon mode of the RADEF Clinac.

TABLE II
PARAMETERS OF THE USED BEAMS AT THE RADEF CLINAC.

Energy (MeV)	Surface dose rate (fraction of max)	Max dose depth (cm H_2O)	S_{coll} (MeV cm^2/g (H_2O))	S_{coll} (MeV cm^2/g (Si))
6	0.78	1.19	1.911	1.639
20	0.91	1.58	2.046	1.796
6 MV [a]	0.47	1.56	-	-

S_{coll} values obtained from [26]
[a] Photon radiation field

(polymethyl methacrylate), and with 2 cm of acrylic below the DUT. This was done so that the dose level in the DUT would correspond to the dose at maximum dose depth in water.

Another factor that was taken into account was the surface homogeneity. No electron applicator was used during the irradiation, which makes the beam surface slightly less homogeneous. The electron fluence at the DUT position was measured to be the fractions 0.79 and 0.88 of the fluence at the beam centre for 6 MeV and 20 MeV electrons respectively, and the presented fluences was corrected with these factors. For the photon mode operation, the inhomogeneities were negligible. The uncertainty of the calculated electron fluence is estimated to be less than 10 %.

The memory dies are encapsulated in a plastic package, and part of the die is covered by the metal bonding. Metal could have an impact on the absorbed dose in the Si die due to dose enhancements present in the interface regions between Si and high-Z materials [27]. The interior design of the memory is not known, in terms of the location of possible metallic material in relation to sensitive die regions. The dose enhancement effect is largest for photons of lower energy, due to the dominance of the photoelectric effect as a photon interaction mode at lower energies. Low energy electrons that are released from the high-Z material can then cause a dose enhancement effect in the interface regions. For higher energy photons, like the ones present here (Fig. 1), this effect is not as big [27]. In this work, the displacement damage effects are also more important than the total dose, and the low energy secondaries are not as important in this regard as the higher energy particles, so no modifications to the value of the absorbed dose was made due to dose enhancement effects.

IV. RESULTS AND DISCUSSION

A. Observed errors

The memory models with smaller node sizes (72 nm and 63 nm, Table I) were only tested at VESPER with 200 MeV electrons. They did not show any response to the energetic electrons during the irradiation, and they were not subjected to irradiation tests with lower energy electrons.

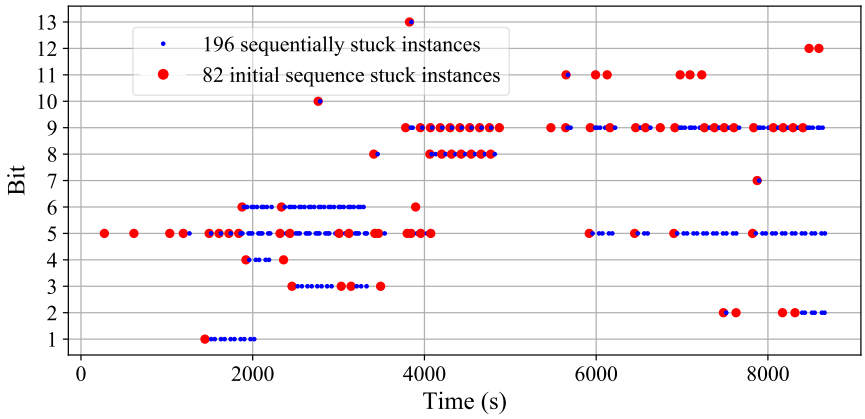

Fig. 2. Time structure of the errors from stuck bits in memory SDF3 under 123 MeV electron irradiation during modified March C- test loops. The bits are numbered as 1 - 13, with each row displaying the behaviour of one of the observed stuck bits.

TABLE III
SUMMARY OF IRRADIATION RESULTS. THE OBSERVED ERRORS OCCURRING BEFORE THE FLUENCE LIMIT IN THE RIGHTMOST COLUMN ARE PRESENTED FOR EACH DUT.

ID	Electron energy (MeV)	Dose rate (rad(Si) /min)	Bit-flips	Stuck bits	Fluence at onset of error rate increase (e/cm^2)
SDF1	200	$1.9 \cdot 10^2$	10	11	$1.58 \cdot 10^{12}$
SDF3	123	$5.6 \cdot 10^2$	10	13	$1.61 \cdot 10^{12}$
SDF4	61	$7.2 \cdot 10^2$	10	13	$3.33 \cdot 10^{12}$
SDF5	20	$5.7 \cdot 10^2$	6	6	$2.78 \cdot 10^{12}$
SDG1	20	$8.2 \cdot 10^2$	2	5	$2.95 \cdot 10^{12}$
SDG3	6	$6.7 \cdot 10^2$	0	0	$2.67 \cdot 10^{12}$
SDG4	20	$2.5 \cdot 10^3$	2	6	$2.43 \cdot 10^{12}$
SDG5	20	$4.1 \cdot 10^2$	4	7	$4.52 \cdot 10^{12}$
SDG6	6 MV [a]	$5.0 \cdot 10^2$	0	0	50 krad(H_2O) [a]
SDB1	200	$1.9 \cdot 10^2$	0	0	$1.0 \cdot 10^{12}$ [b]
SDE1	200	$3.8 \cdot 10^2$	0	0	$1.8 \cdot 10^{12}$ [b]

[a] Tested with 6 MV photon radiation field.
[b] Total fluence on DUT, no errors observed.

During the irradiation tests, two types of errors attributed to SEE were observed in memory type IS42S86400B. One type manifested themselves as bit-flips, which resulted in a single recoverable erroneous read of a bit in a word. The other type was stuck bits. These were bits that returned faulty values more than once, while the bit had been rewritten in between the read operations. They were however generally stuck only for a few write/read cycles. An example of the pattern of errors in the stuck bits can be seen in Fig. 2. In the figure, the red dots represent initial errors, with the previous write and read of the same value in the bit not resulting in an error. The blue dots represent an error in the memory where also the previous write and read cycle of the same value in the bit did give an error. Note that the abscissa of Fig. 2 is irradiation time, since the write/read cycles are periodic in time and the pattern of recurring errors is more clearly visible like this, and is independent of flux fluctuations.

Many of these stuck bits in Fig. 2 were ISBs, i.e. bits that switch between being stuck, and being normally operational. This effect has been discussed e.g. in [13]–[15] with stuck bits observed during irradiation with other particle types than electrons. ISBs discussed in these publications have, like the ones found here, long periods of time where they are not stuck.

The number of detected errors during the tests present a sudden increase at a certain dose level (electron fluence). An example of this is shown in Fig. 3 for the SDF3 memory under 123 MeV electron irradiation after 50 krad(Si). Up to this dose level the errors follow a linear trend with the electron fluence. The same effect was seen in all memories of this model (IS42S86400B), and the point of onset of this error increase is displayed in Table III. The errors up to this point, following a linear trend with the electron fluence, are assumed to originate from SEE induced by the impinging electrons. The number of such errors in each DUT is also presented in Table III.

Similar errors to the electron stuck bit SEEs obersved here, are in e.g. [13], [14] discussed as single particle

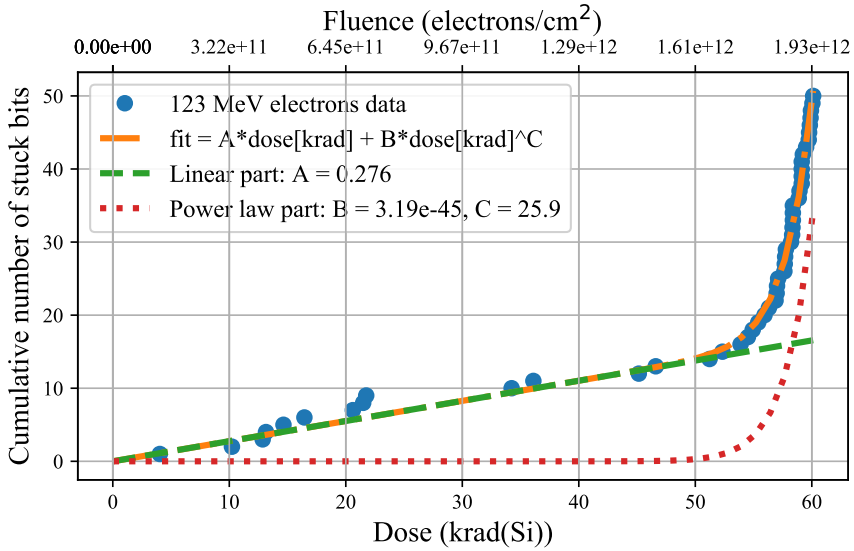

Fig. 3. Errors during irradiation with 123 MeV electrons at VESPER in memory SDF3. The figure shows the onset of new stuck bits in the memory as a function of the surface dose in Si and electron fluence. The trend of new errors has been shown with a fitted function, that is a sum of a linear part and a power law part. The fitting function is $errors = A \cdot dose[krad(Si)] + B \cdot dose[krad(Si)]^C$, where *A*, *B* and *C* are fitted parameters.

displacement damage effects (SPDDEs), where the errors are induced by single protons and neutrons that create damage clusters in a depletion region of the memory cells, increasing the leakage from the stored charge in the cells and causing the bits to become stuck. In [14] a power law dependency on the stuck bits as a function of particle fluence is also discussed, where the exponent (*C* in Fig. 3) according to Poisson statistics correspond to the number of single particle interactions in a sensitive region that are required to cause a stuck bit.

For the 123-MeV electron case in Fig. 3, there is an initial linear slope with single particle interactions causing stuck bits, followed by the error rate increase where around 26 particle interactions are needed to induce the errors. This suggests that rare events induced by single electrons are capable of creating large enough damage clusters to create a stuck bits, while more common, smaller displacement damage complexes can accumulate, and eventually become large enough to also create a stuck bit.

The fitted factor *C* varied between 19 and 37 in the fits to the stuck bit data for all tested IS42S86400B devices. The fitted variable *C* seems to be quite sensitive to the fitting procedure, with fluctuations on the fitted values that were rather independent on particle type and energy, and should rather be viewed as a qualitative measure than an exact numerical value to rely on.

The error rate increase, and the consecutive annealing of the stuck bits discussed later in the paper, present competing effects. In Table III, the reported dose rate is the approximate median for most DUTs, and variations in dose rate occurred during the irradiation. However, in DUTs SDG1, SDG4 and SDG5 the dose rate was kept constant throughout the tests with 20 MeV electrons. The induced stuck bits for the different dose rates in these memories are shown in Fig. 4. In the figure it can be seen that the sharp increase in error rate occurs earlier at higher dose rates, when less time is allowed for the annealing to happen. At a low enough dose rate, the memory might thus not necessarily suffer this kind of break-down from the accumulated damage at all, if the annealing is faster than the damage cluster accumulation.

No SEEs were observed during the tests with 6 MeV electrons or 6 MV photons. Only the error increase due to the cumulative damage was observed. The stuck bits as a function of deposited dose for these tests are shown in Fig. 5. The dose level in this figure is calculated as described in Section III-B, with dose in Si for the electrons, and a water equivalent dose for photons. These results with no errors found before the sharp increase in errors for the cases with low-energy electrons and with photons suggest that these individual particles are not capable of inducing large enough damage clusters to cause stuck bits, but they can still induce smaller damage clusters that may accumulate to large enough complexes which causes the bits to become stuck.

No errors were observed in the IS42S16320D/F memories during the irradiation with 200 MeV electrons. This could be due to a lower error cross section due to the smaller node sizes of the memories, but also due to other design changes between the different memory versions which are unknown to the authors.

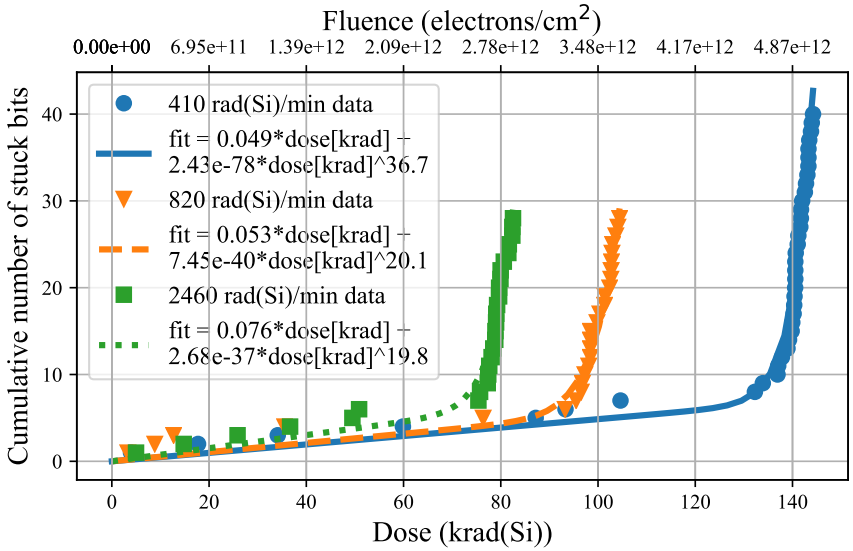

Fig. 4. Stuck bits found in DUTs SDG1, SDG4 and SDG5 at different dose rates of 20 MeV electrons, with fits to the data to show the initial linear region with errors originating from SEE, and the subsequent increase in errors due to the cumulative effects.

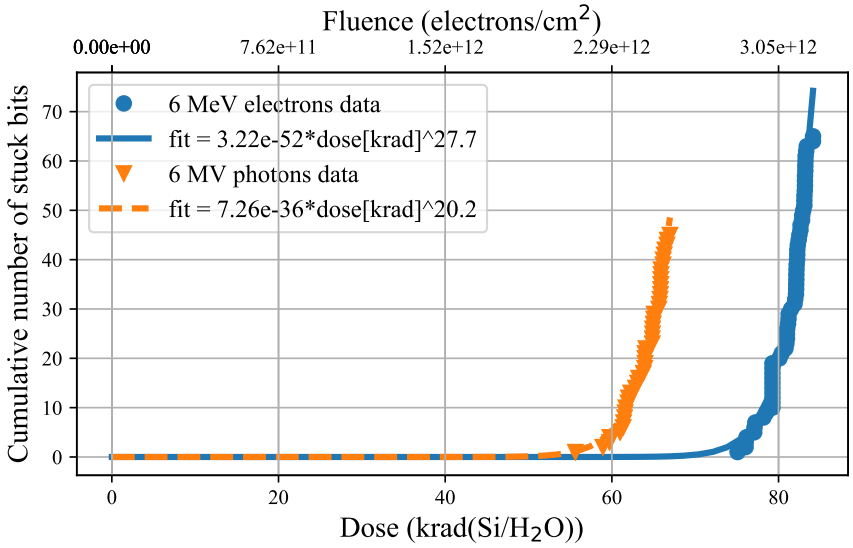

Fig. 5. Stuck bits found in DUTs SDG3 and SDG6 during the tests with 6 MeV electrons and 6 MV photons. Only the sharp increase in errors due to the cumulative damage is seen, and no SEEs before this increase is observed. The dose level is specified in krad(Si) for the electrons and krad(H_2O) for the photons.

B. Stuck bit and single bit-flip cross section

The calculated cross sections for the errors obtained before the increase in error rate are presented in Fig. 6. The error bars in the figure represent a 95 % confidence interval with a 20 % beam fluence uncertainty for the data points at energies over 20 MeV, and 10 % at 20 MeV and below. A similar number of stuck bits and single bit-flips were observed at each of the tested energies, and thus the cross sections for the two failure modes are similar.

In Fig. 6, the 20 MeV point is from the test with SDG1, which was tested at a dose rate of 820 rad(Si)/min. DUTs SDG4, SDG5 and SDF5 were also tested with 20 MeV electron irradiation, but at different dose rates. The resulting SEE cross sections from these tests are shown in Fig. 7, where all tests resulted in similar results for the calculated cross section independent of dose rate, with largely overlapping error bars as would be expected for SEE.

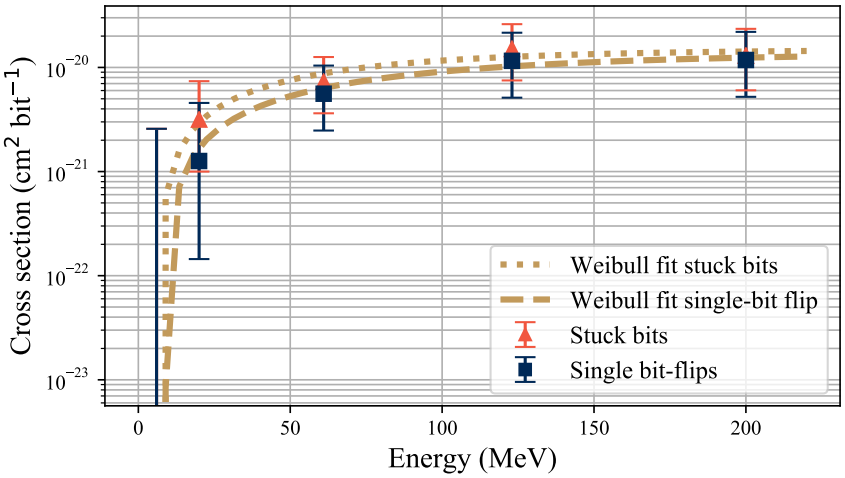

Fig. 6. Stuck bits and single bit-flip cross sections of electron irradiation under dynamic testing. The Weibull fits of the cross sections are also presented, which will be used later for a discussion of the memory behaviour in the Jovian environment. No events were observed for 6 MeV electrons, and only the upper limit is shown.

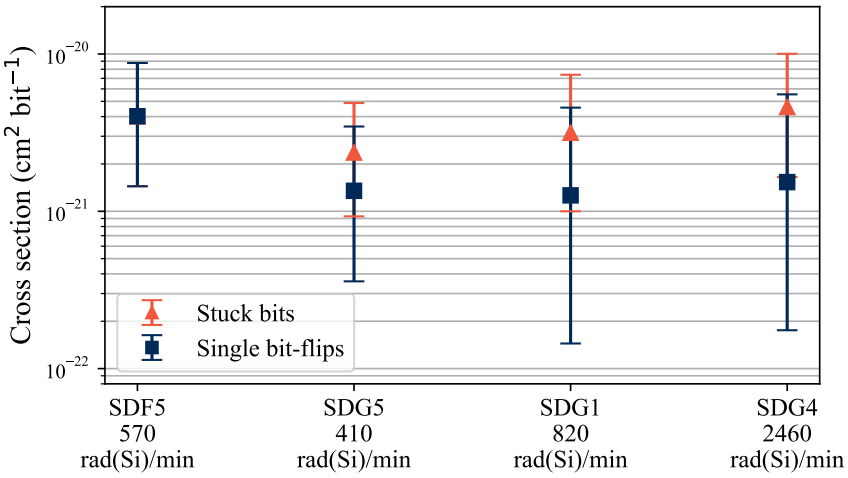

Fig. 7. Stuck bit and single bit-flip cross sections from tests with 20 MeV electrons at different dose rates. The dose rate on DUT SDF5 was varied during the test, while the dose rates for SDG5, SDG1 and SDG4 was kept constant.

C. Damage in memory cells subject to SEE

The bits that are stuck have been damaged by the incident radiation, so that the storage capacitors in the memory cells are not anymore able to hold its charge during the refresh cycles of the memory, and the bits get stuck to their discharged state. For the cells exhibiting single bit-flips, the memory cell storage capacitor has been discharged due to the electron strike, but the cell can still hold the stored charge during the refresh cycles in the following write and read cycles of the test. Fig. 8 shows how the retention time distributions of the cells that have been subject to SEE during irradiation, compared to the total distribution of retention times of all the cells in the memory. This study was made for the memories SDF1, SDF3, SDF4 and SDF5 post-irradiation, with three different cell populations considered in each memory: all cells (All), cells that got stuck during irradiation (Stuck), and cell that exhibited a single bit-flip (Flipped).

The different populations of each memory were for each tested refresh frequency separately checked for failing bits. For the cells that had been subject to SEE during irradiation, the same words which contained the errors during irradiation were written with the same value as when the error occurred (‘0’ or ‘1’) to the memory. One minute later, the data was read back, and the fraction of the population exhibiting errors at the reading of the data is displayed in Fig. 8. The same was done for all words in the memory, where the fraction of the total number of words failing at patterns of either all ‘0’ or all ‘1’ is displayed.

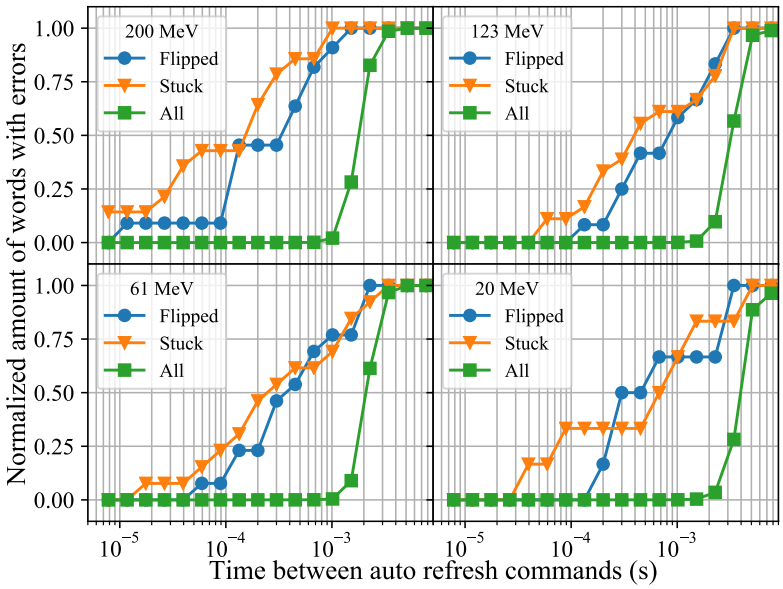

Fig. 8. The amount of words with bits that fail at given refresh frequencies, as a function of auto refresh command frequency of the memory (abscissa is $1/F_R$). The populations that are shown are the bits which had only one bit-flip during irradiation, bits that were stuck, and all bits in the memory. Data taken post irradiation for the four tested SDF# memories (see Table III).

The population of cells that had SEEs fail earlier, at lower refresh frequencies, than the rest of the memory (i.e. all bit population). Also, the population of bits that were stuck during irradiation seem, in general, to fail at lower refresh frequencies than the ones that had a bit-flip. Still, the behaviour of the stuck and the flipped populations, as seen in Fig. 8, are similar.

This can indicate that the mechanisms behind the different failure modes are similar, but differ mainly in the severity. The suggestion that displacement damage caused by single particles creating leakage paths, e.g. in a depletion region common to the storage capacitor and the access transistor [12], [14] (depending on the specific memory layout), is the cause for the stuck bits from SEE in this study is a likely case. This displacement damage would be caused by reaction products from nuclear interactions involving the energetic electrons [8], [9].

Since the cells that exhibited only a single bit-flip display similar behaviour in Fig. 8 to the bits that were stuck, and they display a worse data retention capability than the population of all cells, it is possible that the cause for the single bit-flips found in this study is the same as for the stuck bits. Looking at the behaviour in Fig. 2, some bits are stuck only twice or a few times, while others are stuck in many more instances. It is therefore reasonable that the same kind of failure could result in an error at only one occasion.

D. Retention time distributions and annealing

The retention time distribution of the words in the SDF5 memory during irradiation with 20 MeV electrons is presented in Fig. 9. This figure shows the number of words with bits that are stuck at different refresh frequencies at increasing dose levels. The nominal refresh frequency of the memories, 128 kHz, is marked in the figure with a dotted black line.

These distributions were produced by changing the auto refresh command frequency F_R of the memories (the abscissas in the figures are the inverse of this, $1/F_R$), then writing the memory with all '0' pattern, waiting 60 s, then reading back the memory. Thereafter the procedure was repeated for an all '1' pattern. The sum of the words with errors in these tests is presented on the vertical axis.

The retention time distribution of the words in the SDF5 memory post-irradiation with 20 MeV electrons is presented in Fig. 10, where the annealing of the memory is shown. The memories were kept in room temperature (only room-temperature annealing was performed), and without bias when not characterized. A complete recovery to the pristine case is not observed in the annealing. Instead, the distribution of retention times is approaching one which is shifted upwards, with more words containing failing bits at each measurement point compared to the pristine case. As a comparison, this is the same type of data as is shown in Fig. 8 for the population of all bits in the SDF5 memory.

After the annealing time is in the time-scale of thousands of hours, the amount of errors at lower refresh frequencies start to increase dramatically, while the number of errors at high F_R continues to decrease. This is consistent with

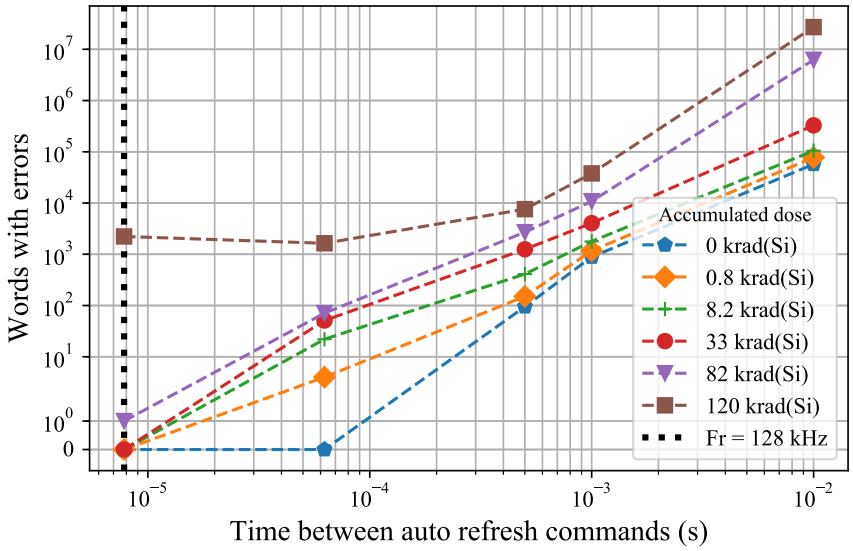

Fig. 9. Retention time distribution of the words in the SDF5 memory during 20 MeV electron irradiation at 5 different refresh frequencies at different deposited doses.

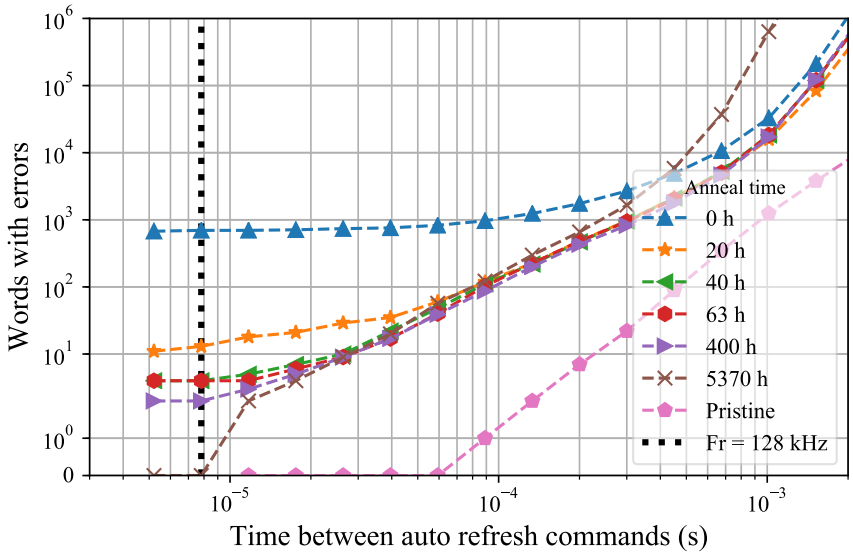

Fig. 10. Retention time distribution of the words in the SDF5 memory after 20 MeV electron irradiation after different annealing times.

results in e.g. [11]. This behaviour, with a continuing decrease of errors at high F_R, and an increase of errors at low F_R after 10^3 h of annealing time, is consistent in the tested memories in this study, both for memories tested with electrons and photons.

The increase in errors at low F_R might be due to an increase of interface traps, accumulating over the annealing time by the access transistor, storage capacitor, or closely located dielectric allowing the storage capacitor to leak its charge faster and reduce the retention time of the bits. At least up to the doses applied in this work, this effect has not been observed to affect the normal operation of the cells at 128 kHz.

V. In-flight predictions

Based on the cross sections presented in Fig. 6, and the expected electron environment during the JUICE mission [1] which is depicted in Fig. 11 along with the cross section Weibull fits, an estimation of the number of upsets the IS42S86400B memory would have during the JUICE mission was made. The mission duration is in total planned to be 11.1 years, with different phases of the mission receiving different fluxes of particles [1].

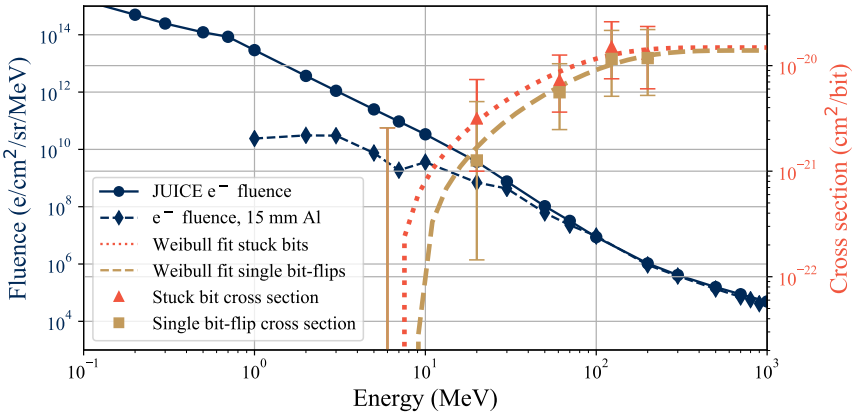

Fig. 11. The total differential electron fluence of the JUICE mission from [1], as well as the transported electron fluence through 15 mm Al. The Weibull fits of the electron cross sections from Fig. 6are also presented.

TABLE IV
ESTIMATED NUMBER OF SEE FROM ELECTRONS IN IS42S86400B DURING THE JUICE MISSION.

Fault	Non-shielded errors	15 mm Al-shielded errors
Stuck bits	2.7	0.6
Single bit-flips	1.1	0.4
Total	3.8	1.0

As an estimation, the presented differential fluence was multiplied with 4π to assume an isotropic radiation field, and also as an approximation an isotropic sensitivity of the component. The component has only been tested with electrons at a normal incidence angle, so the normal incidence angle sensitivity is used for the whole isotropic fluence. The cross section was then folded with the electron fluence over the energies between the cross section cut-off energy and 1 GeV, and multiplied with the number of bits in the memory to obtain an estimation of the number of upsets.

Geant4 was also used to simulate the resulting electron fluence after the original electron fluence had passed through a spacecraft shielding of 15 mm Al. The estimated errors from the shielded and non-shielded electron fluence are shown in Table IV. Due to the low error cross section very few electron-induced SEEs would be expected: 4 for the non-shielded case and 1 for the shielded. In a memory using an error detection and correction system, this low number would not present a problem in the usage.

Shielding thicknesses of 10 mm Al and 14 mm Al during the JUICE mission would result in a TID of 227 krad(Si) and 120 krad(Si) respectively [1], of which a large majority would originate from the trapped electron environment. These doses would translate to average dose rates of about 39 mrad(Si)/min and 21 mrad(Si)/min, instead of the $10^2 - 10^3$ rad(Si)/min which was used in the testing in this work. The memory tested at the lowest dose rate 410 rad(Si)/min in Fig. 4 failed due to the accumulated radiation damage after about 130 krad(Si). However, with the much lower dose rate encountered on the JUICE mission, it is not clear if the small damage clusters would anneal before accumulating and being capable to induce stuck bits even at 227 krad(Si). If a thicker shielding than 10 mm Al is used (e.g. 14 mm), then the mission dose values are comparable to the ones reached during some of the tests presented here.

VI. CONCLUSION

In this paper, high-energy electron irradiation is demonstrated to cause stuck bits and bit-flips in SDRAMs as SEEs, and cross sections for these failure modes are determined. These cross sections are put in relation to the Jovian environment, and a number of expected SEEs from electrons if the memory was to be used on the JUICE mission is estimated. The estimated number is low, 3.8 in total, and electron-induced SEEs are not expected to be a large problem if the memory is to be used on the mission.

The mechanism behind the two observed SEE failure modes stuck bits and single bit-flips is suggested to be the same. This is based on the similarity of the degraded retention time distributions of the cell populations consisting of bits that were stuck, and those that had bit-flips, compared to that of the total cell population.

The electron irradiation is found to degrade the memory cells on a long time scale. Annealing of the cell damage was observed, but also an increase in failing cells at low refresh rates was observed after long annealing times.

In these accelerated tests, where high dose rates and electron fluxes were utilized, a sharp increase in the number of errors in the memory was observed. This effect is attributed to the accumulation of smaller damage clusters, and occurs at lower dose levels for higher dose rates, when less time is allowed for annealing in between events.

To estimate the total performance of the memory in the JUICE environment, it would be needed to perform tests at low electron fluxes and dose rates. This because of the dose rate dependence on the memory response observed in this study. The temperatures effect on the annealing properties would also have to be investigated to be able to predict the memory response on board JUICE.

REFERENCES

[1] JUICE Team, "JUICE environment specification," European Space Agency (ESA)/ESTEC, Revision 5 Issue 5, Feb. 2017, reference JS-14-09.

[2] I. de Pater and D. E. Dunn, "VLA observations of Jupiter's synchrotron radiation at 15 and 22 GHz," *Icarus*, vol. 163, no. 2, pp. 449–455, Jun. 2003, doi: https://doi.org/10.1016/S0019-1035(03)00068-X.

[3] M. de Soria-Santacruz, H. B. Garrett, R. W. Evans, I. Jun, W. Kim, C. Paranicas, and A. Drozdov, "An empirical model of the high-energy electron environment at Jupiter," *J. Geophys. Res. Space Phys.*, vol. 121, no. 10, p. 9732–9743, Oct. 2016, doi: https://doi.org/10.1002/2016JA023059.

[4] M. P. King, R. A. Reed, R. A. Weller, M. H. Mendenhall, R. D. Schrimpf, B. D. Sierawski *et al.*, "Electron-induced single-event upsets in static random access memory," *IEEE Trans. Nucl. Sci.*, vol. 60, no. 6, pp. 4122–4129, Dec. 2013, doi: 10.1109/TNS.2013.2286523.

[5] A. Samaras, P. Pourrouquet, N. Sukhaseum, L. Gouyet, B. Vandevelde, N. Charty *et al.*, "Experimental characterization and simulation of electron-induced SEU in 45-nm CMOS technology," *IEEE Trans. Nucl. Sci.*, vol. 61, no. 6, pp. 3055–3060, Dec. 2014, doi: 10.1109/TNS.2003.820727.

[6] M. J. Gadlage, A. H. Roach, A. R. Duncan, M. W. Savage, and M. J. Kay, "Electron-induced single-event upsets in 45-nm and 28-nm bulk CMOS SRAM-based FPGAs operating at nominal voltage," *IEEE Trans. Nucl. Sci.*, vol. 62, no. 6, pp. 2717–2724, Dec. 2015, doi: 10.1109/TNS.2015.2491220.

[7] J. M. Trippe, R. A. Reed, R. A. Austin, B. D. Sierawski, R. A. Weller, E. D. Funkhouser *et al.*, "Electron-induced single event upsets in 28 nm and 45 nm bulk SRAMs," *IEEE Trans. Nucl. Sci.*, vol. 62, no. 6, pp. 2709–2716, Dec. 2015, doi: 10.1109/TNS.2015.2496967.

[8] M. Tali, R. G. Alía, M. Brugger, V. Ferlet-Cavrois, R. Corsini, W. Farabolini *et al.*, "High-energy electron-induced SEUs and jovian environment impact," *IEEE Trans. Nucl. Sci.*, vol. 64, no. 8, pp. 2016–2022, Aug. 2017, doi: 10.1109/TNS.2017.2713445.

[9] ——, "Mechanisms of electron-induced single-event latchup," *IEEE Trans. Nucl. Sci.*, vol. 66, no. 1, pp. 437–443, Jan. 2019.

[10] H. Shindou, S. Kuboyama, N. Ikeda, T. Hirao, and S. Matsuda, "Bulk damage caused by single protons in SDRAMs," *IEEE Trans. Nucl. Sci.*, vol. 50, no. 6, pp. 1839–1845, Dec. 2003, doi: 10.1109/TNS.2003.820727.

[11] J. P. David, F. Bezerra, E. Lorfèvre, T. Nuns, and C. Inguimbert, "Light particle-induced single event degradation in SDRAMs," *IEEE Trans. Nucl. Sci.*, vol. 53, no. 6, pp. 3544–3549, Dec. 2006, doi: 10.1109/TNS.2006.886210.

[12] L. D. Edmonds and L. Z. Scheick, "Physical mechanisms of ion-induced stuck bits in the hyundai 16M x 4 SDRAM," *IEEE Trans. Nucl. Sci.*, vol. 55, no. 6, pp. 3265–3271, Dec. 2008, doi: 10.1109/TNS.2008.2006902.

[13] A. M. Chugg, J. McIntosh, J. Burnell, P. H. Duncan, and J. J. Ward, "Probing the nature of intermittently stuck bits in dynamic RAM cells," *IEEE Trans. Nucl. Sci.*, vol. 57, no. 6, pp. 3190–3198, Dec. 2010, doi: 10.1109/TNS.2010.2084103.

[14] A. M. Chugg, A. J. Burnell, P. H. Duncan, S. Parker, and J. J. Ward, "The random telegraph signal behavior of intermittently stuck bits in SDRAMs," *IEEE Trans. Nucl. Sci.*, vol. 56, no. 6, pp. 3057–3064, Dec. 2009, doi: 10.1109/TNS.2009.2032184.

[15] V. Goiffon, T. Bilba, T. Deladerrière, G. Beaugendre, A. Le-Roch, A. Dion *et al.*, "Radiation induced variable retention time in dynamic random access memories," *IEEE Trans. Nucl. Sci.*, vol. 67, no. 1, pp. 234–244, Jan. 2020, doi: 10.1109/TNS.2019.2956293.

[16] A. Samaras, B. Vandevelde, N. Sukhaseum, N. Charty, A. Rodriguez, F. Wrobel *et al.*, "Experimental characterization and in-flight observation of weakened cell in SDRAM," in *2015 15th European Conference on Radiation and Its Effects on Components and Systems (RADECS)*, 2015, doi: 10.1109/RADECS.2015.7365611.

[17] ISSI, *IS42S86400B, IS42S16320B, IS45S16320B - 64M x 8, 32M x 16, 512Mb SYNCHRONOUS DRAM, Rev. H*, Integrated Silicon Solution, Inc., Dec. 2011, accessed on: August 31, 2020. [Online]. Available: http://www.issi.com/WW/pdf/42S16320B-86400B.pdf

[18] ——, *IS42/45R86400D/16320D/32160D IS42/45S86400D/16320D/32160D - 16Mx32, 32Mx16, 64Mx8 512Mb SDRAM, Rev. B*, Integrated Silicon Solution, Inc., May 2015, accessed on: October 1, 2020. [Online]. Available: http://www.issi.com/WW/pdf/42-45R-S_86400D-16320D-32160D.pdf

[19] ——, *IS42R86400F/16320F, IS45R86400F/16320F, IS42S86400F/16320F, IS45S86400F/16320F - 32Mx16, 64Mx8 512Mb SDRAM, Rev. B1*, Integrated Silicon Solution, Inc., Jul. 2017, accessed on: October 1, 2020. [Online]. Available: http://www.issi.com/WW/pdf/42-45R-S_86400F-16320F.pdf

[20] Terasic, *DE0-CV User Manual*, Terasic Inc., May 2015, accessed on: October 1, 2020. [Online]. Available: https://www.terasic.com.tw/cgi-bin/page/archive.pl?Language=English&CategoryNo=167&No=921&PartNo=4

[21] L. Dilillo, G. Tsiligiannis, V. Gupta, A. Bosser, F. Saigne, and F. Wrobel, "Soft errors in commercial off-the-shelf static random access memories," *Semiconductor Science and Technology*, vol. 32, no. 1, p. 013006, dec 2016, doi: 10.1088/1361-6641/32/1/013006.

[22] K. Sjobak, E. Adli, C. A. Lindstrom, M. Bergamaschi, S. Burger, R. Corsini *et al.*, "Status of the CLEAR Electron Beam User Facility at CERN," in *Proc. 10th International Particle Accelerator Conference (IPAC'19), Melbourne, Australia, 19-24 May 2019*, ser. International Particle Accelerator Conference, no. 10, Geneva, Switzerland, Jun. 2019, pp. 983–986, https://doi.org/10.18429/JACoW-IPAC2019-MOPTS054.

[23] H. Kettunen, *Varian Clinac linear accelerator*, University Of Jyväskylä, Aug. 2020, accessed on: October 1, 2020. [Online]. Available: https://www.jyu.fi/science/en/physics/research/infrastructures/research-instruments/miscellaneous-instruments/clinac

[24] S. Agostinelli, J. Allison, K. Amako, J. Apostolakis, H. Araujo, P. Arce *et al.*, "Geant4—a simulation toolkit," *Nucl. Instrum. Methods Phys. Res. A, Accel. Spectrom. Detect. Assoc. Equip.*, vol. 506, no. 3, pp. 250–303, 2003.

[25] IBA, *DETECTORS For Relative and Absolute Dosimetry - Ionization chambers and diode detectors*, IBA Dosimetry, 2018, accessed on: October 1, 2020. [Online]. Available: https://www.iba-dosimetry.com/fileadmin/user_upload/products/02_radiation_therapy/_Detectors/Detectors-RD-_-AD_Rev.3_0718_E.pdf

[26] M. J. Berger, J. S. Coursey, M. A. Zucker, and J. Chang, "Stopping-power & range tables for electrons, protons, and helium ions," NIST, Physical Measurement Laboratory, NIST Standard Reference Database 124 NISTIR 4999, Jul. 2017, DOI: https://dx.doi.org/10.18434/T4NC7P.

[27] D. M. Long, D. G. Millward, R. L. Fitzwilson, and W. L. Chadsey, "Handbook for dose enhancement effects in electronic devices," P.O. Box 2351, La Jolla Ca 92038, Tech. Rep. RADC-TR-83-84, Mar. 1983.